UNIVERSALITY OF PROBABILITY DENSITY FUNCTION OF VELOCITY FLUCTUATION IN HIGH-REYNOLDS NUMBER WALL-BOUNDED SHEAR FLOW

Yoshiyuki Tsuji
Department of Energy Engineering and Science
Nagoya University
Chikusa-ku, Nagoya, 464-8603, Japan
Email:c42406a@nucc.cc.nagoya-u.ac.jp

Yoshinobu Yamamoto
Department of Mechanical Engineering,
University of Yamanashi,
Kofu 400-8511, Japan

Marie Ono
National Institute of Advanced Industrial Science and Technology (AIST), National Metrology Institute of Japan(NMIJ),1497-1 Teragu, Tsukuba, Japan

Noriyuki Furuichi
National Institute of Advanced Industrial Science and Technology (AIST), National Metrology Institute of Japan(NMIJ),1497-1 Teragu, Tsukuba, Japan

ABSTRACT

Probability density function (PDF) of streamwise velocity component is studied in canonical wall-bounded flow (Channel, Pipe, and Boundary layer). When normalized by the mean and standard deviation, the PDF of the fluctuations exhibits invariance within distinct wall-normal regions. Two such regions were identified: one situated near the plateau of the turbulence intensity profile, and the other associated with the logarithmic region consistent with Townsend's attached-eddy hypothesis. The PDF shapes in both regions are independent of Reynolds number, demonstrating their universality.

INTRODUCTION

In wall-bounded shear flows, several studies have examined the universality of the PDF shape in channel flows (Dinavahi et al. (1995)) and turbulent boundary layers (Tsuji & Nakamura (1999)). When velocity fluctuations are normalized by their mean and standard deviation, it has been reported that PDF shapes become universal in certain regions away from the wall. These results were first obtained at low Reynolds numbers, but the same idea was later verified at relatively high Reynolds numbers by Lindgren et al. (2004) and Zhou & Klewicki (2015). Lindgren et al. (2004) reported that the self-similar PDF region extends beyond the universal overlap region, starting at $y^+ \simeq 160$ and reaching out to 0.3δ. Zhou & Klewicki (2015) found that the self-similar region is estimated to lie within the bounds $2.6\sqrt{\delta^+}$ and $0.3\delta^+$, which are inside the bounds of the self-similar inertial domain associated with the mean momentum equation. Here, δ is the boundary layer thickness, + indicates the inner normalization.

From the above brief review of PDF studies in turbulent boundary layers, it is still not clearly understood how the PDFs vary at higher Reynolds numbers ($O(10^4) \leq R_\tau$), whether universal shapes appear, and where they are realized. In this paper, we investigate the PDF of streamwise velocity fluctuations in a zero-pressure-gradient turbulent boundary layer at first, while taking into account the spatial resolution of the hot-wire probe. By analyzing PDF shapes across the boundary layer, we identify the invariant PDF region, where the shape does not change, and clarify where it becomes universal, independent of Reynolds number. Finally, we discuss the relation between the invariant PDF region and the log-law region of the mean velocity and turbulence intensity. The invariant PDF shape and its universality is examined in channel and pipe flow.

FLOW FIELD

Boundary layer

The velocity fluctuation in high-Reynolds number zero-pressure-gradient turbulent boundary layers was measured by single hot-wire in RTRI (Railway Technical Research Institute) low-noise wind tunnel in Maibara Japan. The wind tunnel was constructed to promote research and development on aerodynamic noise and other subjects related to Shinkansen and other high-speed railways (see Fig.1). The closed test section, 5m width × 3m height × 20m length. The flat plate is placed inside the test section and the fluctuating stream-wise velocity component is measured by a constant temperature anemometry with I-type probe at the position 6.0, 14.4 and 18.7m from the leading edge. The mean skin friction is determined using oil-film interferometry. As the detailed experimental conditions are mentioned in Tsuji et al. (2021).

The momentum thickness Reynolds number $R_\theta \equiv U_0\theta/\nu$, where θ is momentum thickness, U_0 is free-stream velocity, and ν is kinematic viscosity is up to $R_\theta \cong 8.4 \times 10^4$. Or the friction Reynolds number $R_\tau \equiv u_\tau\delta/\nu$ is $R_\tau \cong 2.6 \times 10^4$ (here, u_τ is friction velocity).

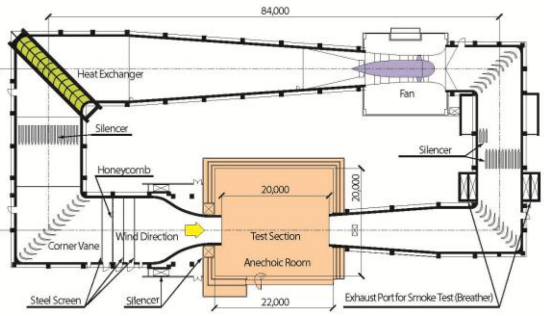

Fig. 1 Plane view of wind tunnel facility at RTRI wind tunnel technical center (http://www.rtri.or.jp/rd/maibara-wt/INDEX.HTML). The unit of length is mm.

Pipe flow

Experiments were conducted in the High Reynolds Number Actual Flow Facility (Hi-Reff, in Fig.2), which uses water as the working fluid (Furuichi et al., 2015). Hi-Reff is equipped with an overflow head tank that provide a stable flow to the test section, a large-capacity underground storage tank to maintain stability water temperature, and a static gravimetric weighing tank for highly accurate flow rate measurement. The straight pipe, with a diameter D=100 mm, has a length of 110 D, of which 90D is carefully polished to achieve a mean roughness of Ra=0.1 μm. Downstream of the polished section, a window chamber containing a glass pipe was installed. The glass pipe is also meticulously polished to ensure high roundness of the inner diameter and a minimal tolerance in wall thickness. Velocity measurements were conducted by laser Doppler velocimetry (LDV). By varying the beam orientation and the measurement line, and all three velocity components were measured (Ono et al., 2023). The fringe distance created by the crossing of split beams and the size of the measurement volume are critical factors for ensuring measurement accuracy. The Reynolds number achieved was up to R_τ=20750.

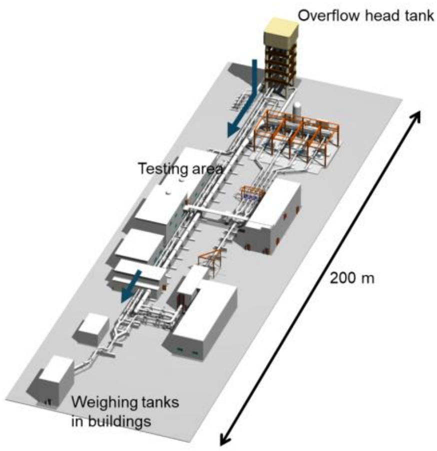

Fig. 2 High Reynolds Number Actual Flow Facility at National Institute of Advanced Industrial Science and Technology (AIST).

Channel Flow

Channel flow data were obtained from direct numerical simulation (DNS, instantaneous velocity fluctuation is shown in Fig.3). The flow is an incompressible fluid that obeys the Naiver-Stokes equation and the incompressibility condition under a constant mean pressure gradient (Yamamoto et al, 2018). The DNS was carried out on 138,240 nodes (6,635,520 cores) of the supercomputer Fugaku at the RIKEN Center for Computational Science. The Reynolds number achieved was up to $R\tau$=15985.

RESULTS AND DISCUSSIONS

The probability density function (pdf) shapes of streamwise component are carefully analyzed, and one of the measures characterizing pdf is introduced. It is the Kullback-Leibler divergence (KLD) or relative entropy. This measure, which was introduced by Kullback (1959) and adopted as a basic quantity in the information theory, is defined as follows:

$$D(P||Q) \equiv \sum_{\{s\}} P(s_i)\ln\{P(s_i)/Q(s_i)\} \tag{1}$$

where $P(\boldsymbol{s})$ and $Q(\boldsymbol{s})$, $\{\boldsymbol{s}\} = \{s_1, s_2, s_3 \cdots\}$ are discrete probability distributions. KLD has a non-negative value for any $P(\boldsymbol{s})$ and $Q(\boldsymbol{s})$, and it is zero only when $P(\boldsymbol{s})$ is exactly equal to $Q(\boldsymbol{s})$. The more the $P(\boldsymbol{s})$ and $Q(\boldsymbol{s})$ come to resemble each other, the smaller is the KLD. Thus KLD indicates quantitatively the resemblance between $P(\boldsymbol{s})$ and $Q(\boldsymbol{s})$. In this analysis, $Q(\boldsymbol{s})$ is taken to be Gaussian distribution and $P(\boldsymbol{s})$ is set to the pdf measured at distance y from the wall. The instantaneous velocity of streamwise component is decomposed into mean and fluctuation as $\tilde{u} = U + u'$. The normalized velocity $u \equiv u'/u_r$, where u_r is a standard deviation of u' is focused on in this analysis (Furuichi, 2025).

Invariant PDF regions

Figure 4 shows the mean velocity, KLD, and turbulence intensity distributions. The mean velocity profile follows the log-law relation, plotted as a solid line, $U^+ = 1/\kappa \ln(y^+) + B$, where $\kappa = 0.384$ and $B = 4.17$ are the values suggested by Nagib & Chauhan (2008). The solid lines agree well with the present measurements. The Kullback–Leibler divergence (KLD) varies with distance from the wall. It reaches a minimum at $y^+ \simeq 50$, indicating that at this location the probability density of u most closely resembles a Gaussian distribution among the measured PDFs. Where the KLD remains constant, the PDF shapes do not change; this corresponds to the invariant PDF region. It is confirmed that the probability density functions of stream-wise velocity fluctuation become invariant in two different locations. They are called pdf invariant region **I** and invariant region **II**, respectively. Two invariant regions exist only for high Reynolds numbers at $R_\tau \simeq O(10^4)$. When two invariant pdf regions appear, the mean velocity is approximated sufficiently by the logarithmic profiles $U^+ = \kappa^{-1}\ln(y^+) + B$ with constant κ and B in $200 \lesssim y^+ \lesssim 0.2\delta^+$. Two invariant regions are contained inside this mean flow log-law region. Kármán constant κ and additive constant B are evaluated as $\kappa = 0.385 \pm 0.003$, $B = 4.26 \pm 0.15$, respectively.

Turbulent intensity distribution

On the turbulent intensity profile, there is another log-law derived from Townsend's attached eddy hypothesis; $(u_r^+)^2 = A_u \ln(y/\delta) + B_u$. This relation is observed only in very high Reynolds number. The question of whether A_u depends on Reynolds number appears to be closely related to the definition of the log-law region used to evaluate its slope, even at high Reynolds numbers. According to the self-similar concept of Townsend's attached-eddy picture, the log-law

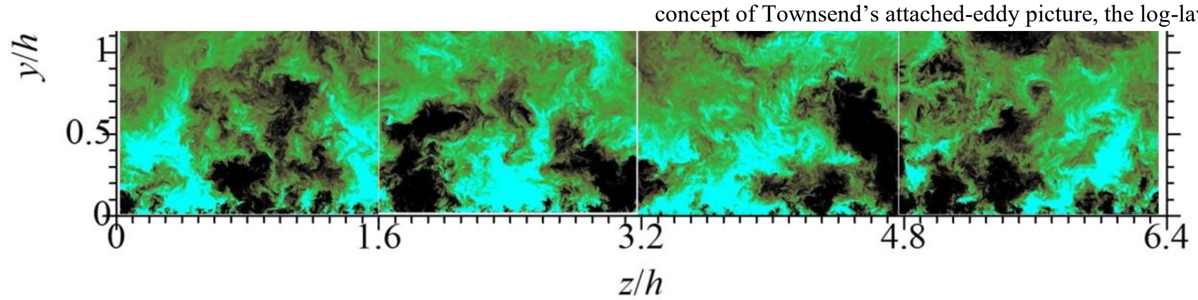

Fig. 3 Contour plots of u of DNS from end view, at $R_\tau \simeq 16000$, -3(black) < u^+ < 3(green).

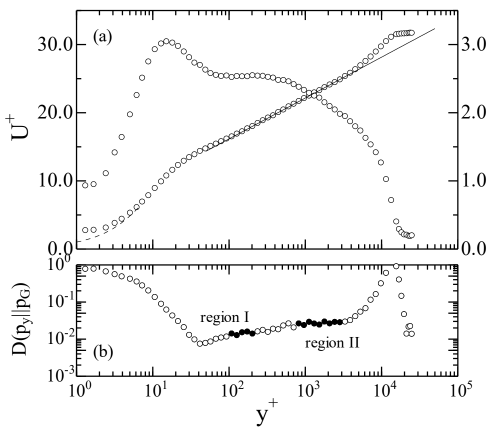

Fig. 4 (a)Mean velocity and turbulent intensity profiles normalized by inner variables at $R_\tau = 15070$ of turbulent boundary layer. Solid line represents log-law relation. (b)KL-divergence distribution defined by Eq.(1). Solid symbols are invariant pdf regions.

region may be identified with the region of self-similar PDFs, i.e. the invariant PDF region. At high Reynolds numbers, invariant PDF region **II** emerges, and we assume that this region is appropriate for the log-law region of the attached-eddy picture. In Fig. 5, the start and end locations of invariant region II are normalized by δ. The ratio remains nearly constant, and invariant region **II** can be evaluated as $0.07 \lesssim y/\delta \lesssim 0.2$ for large Reynolds numbers ($O(10^4) < R_\tau$). At lower Reynolds numbers, the data exhibit slight scatter because invariant region **II** does not appear clearly. By fitting the log law relation: $(u_r^+)^2 = A_u \ln(y/\delta) + B_u$ to invariant PDF region **II**, the slope A_u and constant B_u were calculated. The results are shown in Fig. 6. Both A_u and B_u appear to remain constant for large Reynolds numbers ($O(10^4) < R_\tau$), with values of $A_u \simeq 1.42$ and $B_u \simeq 1.75$. These values are slightly larger than those reported previously, but they are of the same order of magnitude. It should be emphasized that A_u and B_u are determined here from clearly defined regions. If the fitting region is not objectively specified, the slope and additive constant cannot be uniquely determined.

Channel and pipe flow

In comparisom of these pdf invariant properties in zero-perssure gradient turbulent bounadry layer with those of channel and pipe flow, there are two invariant PDF regions. One situated near the plateau of the turbulence intensity profile, and the other associated with the logarithmic region consistent with Townsend's attached-eddy hypothesis.

KLD distribution of channel is very similar with that of pipe except the center region. KLD in pipe indicates the smaller value than in channel. Therefore, the PDF in pipe is closer to Gaussian. There are two invariant PDF regions. One is close to that of boundary layer, however the second invariant region locates outer than that of boundary later. KLD has smaller value in PDF region **I**, but has larger value in PDF region **II** than those of boundary layer. These difference may be attribute to the distinct interaction between inner and outer motions. Even in the present high-Re number, outer scale (or large scale motions) affects the inner regions, and the scale separation is not satisfied.

By fitting the log law relation: $(u_r^+)^2 = A_u \ln(y/\delta) + B_u$ to invariant PDF region **II**, the slope A_u and constant B_u were calculated. As the experimental data were sampled at discrete sampling points, the local slope is not easy to calculate. Judging from the comparison among $(u_r^+)^2$ distributions of three flow fields, there is no large difference of A_u. But B_u depends the flow field because the definition of δ is not the same among them. The details will be discussed at the presentation.

Spectra in the invariant PDF regions

According to Townsend's original idea and the model by Perry et al (1986), the spectra of streamwise velocity component indicate the power law of -1 slope in the log-region of $(u_r^+)^2$. However, this trend was not observed in the present high Reynolds number data. The -1 power law was observed in invariant PDF region **I**, and the Kolmogorov's -5/3 spectra was confirmed in invariant region **II.**

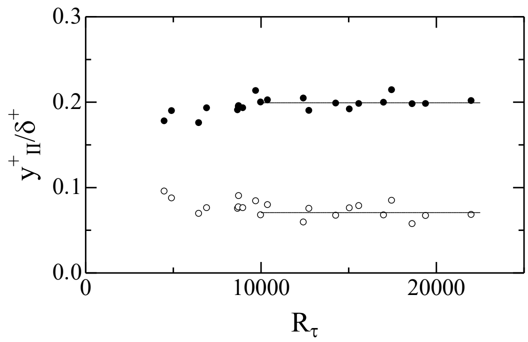

Fig. 5 Start and end locations of invariant PDF region **II** normalized by the boundary-layer thickness.

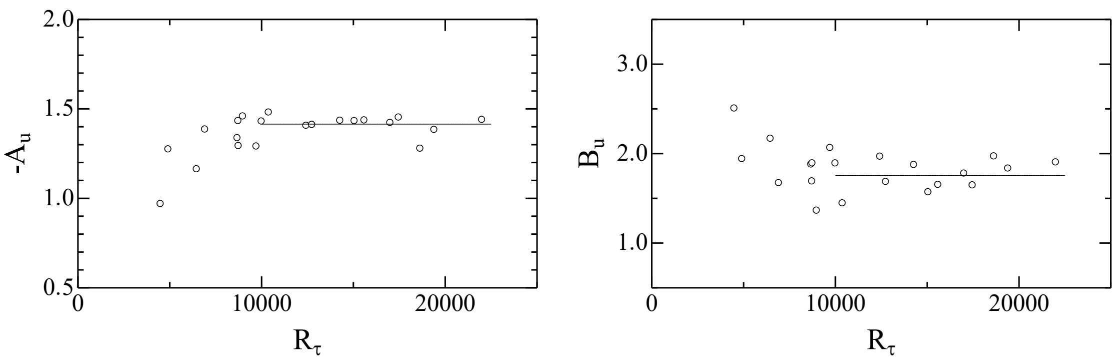

Fig. 6 Slope of the turbulence intensity profile, A_u, and additive constant, B_u, obtained by fitting $(u_r^+)^2 = A_u \ln(y/\delta) + B_u$ over invariant PDF region **II** of turbulent boundary layer.

REFERENCE

Dinavahi, S. P. G., Breuer, K. S., and Sirovich, L. (1995), Universality of probability density functions in turbulent channel flow. Physics of Fluids 7, pp. 1122–1129.

Furuichi, N., Terao, Y., Wada, Y., Tsuji, Y., (2015), Friction factor and mean velocity profile for pipe flow at high Reynolds numbers. Phys. Fluids, 27(9).

Furuichi, N., Ono, M., Tsuji, Y., (2025), Self-similarity in the logarithmic region of turbulence intensity in high-Reynolds-number pipe flow, Int. J. Heat and Fluid Flow, Vol.115, 109836.

Kullback, S., Information Theory and Statistics, (1959), Wiley, London.

Lindgren, B., Johansson, A. V. and Tsuji, Y., (2004), Universality of probability density distributions in the overlap region in high reynolds number turbulent boundary layers. Phyics of Fluids 16, pp. 2587–2591.

Nagib, H. M. and Chauhan, K. A., (2008), Variations of von kármán coefficient in canonical flows, Phys. Fluids 508 41, 021404(23pp).

Ono, M., Furuichi, N., Tsuji, Y., (2023), Reynolds number dependence of turbulent kinetic energy and energy balance of the 3-component turbulence intensity in a pipe flow, *J. Fluid Mech.* **975**, A9.

Perry, A. E., Henbest, S., and Chong, M. S., (1986), A theoretical and experimental study of wall turbulence, J . Fluid Mech., vol. 165, pp.163-199.

Tsuji, Y. and Nakamura, I., (1999), Probability density function in the log-law region of low Reynolds number turbulent boundary layer, *Phys. Fluids* **11**, pp. 647–658.

Tsuji, Y., IDO, A., and Nishioka, M., (2021), Universality of mean velocity profile in high Re-number turbulent boundary layer, Trans. of the JSME, vol.87, p. 21-00280 (in Japanese).

Townsend, A., The Structure of Turbulent Shear Flow (2nd ed.), (1976), Cambridge University Press.

Yamamoto, Y. and Tsuji, Y., (2018), Numerical evidence of logarithmic regions in channel flow at Re_τ= 8000, *Phys. Rev. Fluids,* vol. 3, no. 1, 012602.

Zhou, A. and Klewicki, J., (2015), Properties of the streamwise velocity fluctuations in the inertial layer of turbulent boundary layers and their connection to self-similar mean dynamics, Int. J. Heat and Fluid Flow, 548 51, pp. 372–382.